Thermomechanical Fatigue Resistance of Low Temperature Solder for Multiwire Interconnects in Photovoltaic Modules

Laura Spinella*[a] and Nick Bosco[a]

[a]National Renewable Energy Laboratory, 15013 Denver W Pkwy, Golden, CO 80401 USA
**Corresponding author. E-mail: laura.spinella@nrel.gov*

ABSTRACT

Novel interconnect technologies leveraging low melting temperature solders, such as multiwire interconnects, are being deployed in photovoltaic (PV) modules for improved reliability through interconnect redundancy and lower thermal loads during interconnection and lamination. However, the equivalency of standardized accelerated testing to field conditions has not yet been established for these emerging technologies. In this study, the thermomechanical fatigue resistance of low temperature solder alloys is investigated and compared to that of conventional SnPb to assess the acceleration behavior of these alloys. While InSn is shown to have sufficient thermomechanical fatigue resistance on the order of that of SnPb, these results indicate Sn-Bi alloys may have poor thermomechanical fatigue resistance at field conditions. The results also show that Sn-Bi alloys have thermal cycling acceleration factors of less than one. This indicates that the standardized accelerated thermal cycling test, such as that in IEC 61215, will produce misleading results for Sn-Bi alloys and that unique testing is required for this PV module architecture. Though accelerated thermal cycling may be a meaningful qualification test for Sn-Pb solder joints, these results suggest that mechanical loading may be a more appropriate test for Sn-Bi multiwire interconnects. This is due to the distinct processing and geometry of multiwire interconnects which may allow for mechanical, rather than strictly metallurgical interconnections.

Keywords—accelerated testing, multiwire, durability, indium, bismuth, low temperature solder

1. Introduction

The prevalent interconnect technology in photovoltaics (PV) is currently solder-coated ribbons, where the solder is a lead-based alloy and is reflowed for metallurgical bonding before lamination of the module. Sn-Pb and lead-free solder alloys, such as Sn-Ag-Cu (SAC) have been explored extensively, such that the material parameters and their temperature dependences are well known and include quantification of creep, fatigue behavior and the effects of material aging [1, 2]. Sn-Pb and SAC solders have been investigated in PV applications with both models and field studies and have been shown to fail via thermomechanical fatigue [3, 4, 5, 6]. However, lesser-understood low temperature solders such as indium and bismuth-based alloys are also being implemented for a variety of PV applications, such as multiwire interconnect designs like commercial SmartWire Connection Technology (SWCT) from Meyer Burger or the TWILL-BIPV research project from imec [7]. Multiwire designs use polymer foils embedded with 12-18 narrow copper wires coated in a low temperature solder. Earlier generations used In-Sn alloys, but due to high cost, Sn-Bi alloys are now more dominant [8]. As shown in Fig. 1, these foils are aligned on the cells and laminated, such that the interconnects are formed as the solder reflows at typical lamination temperatures [9]. This interconnect design offers increased interconnect redundancy, lower thermal loads on the cell during interconnection and lamination, lower Ag consumption, and reduced shading and ohmic losses leading to both improved reliability and improved performance [8]. Due to the lower thermal stresses during processing, multiwire is being investigated for flexible PV where the cells are significantly thinner [10] and for heterojunction cell technologies (SHJ) where the cells are more sensitive to temperature [11]; due to the improved aesthetics, multiwire is being investigated for building integrated PV (BIPV) [7]. Studies employing low temperature solder alloys for shingled cell applications are also emerging as an alternative to electrically conductive adhesives (ECAs) [12].

However, initial studies of In-Sn and Sn-Bi alloys indicate shorter mechanical fatigue lifetimes than eutectic SnPb [13, 14], despite results indicating that the addition of an alloying element to Sn-Bi, such as Ag, in small amounts may increase wettability and extend the fatigue lifetime to nearer that of SnPb [15]. For multiwire PV using low temperature alloys, cracking of the solder joint has been observed in a commercial module subjected to dynamic mechanical loads, Fig. 2. The thermomechanical fatigue of the low temperature alloys has not been investigated for the longer timescales required of PV modules, nor have failure modes been extensively explored for multiwire modules. Furthermore, standardized accelerated testing, such as IEC 61215, which is widely used to screen module designs for early failure mechanisms, was developed for conventional SnPb with few soldered busbars. Thus, it is unlikely that these same tests will be an appropriate choice for low temperature solder joints in multiwire interconnects or shingled cells. This is due to the considerable material differences in stiffness, microstructure, and temperature sensitivity, as well as distinct geometries and processing from conventional PV modules.

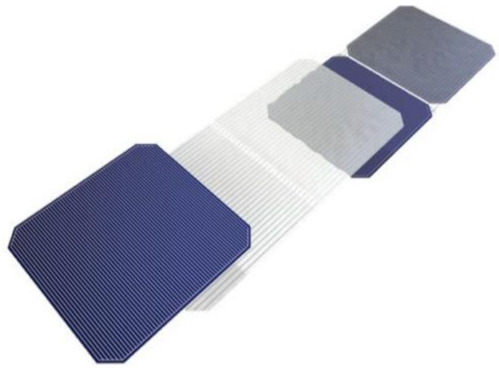

Fig. 1. Schematic of alignment of multiwire foils on cells prior to lamination *[9]*. The interconnects are formed during lamination due to the low melting point of the solder, reducing thermal stresses to the cell.

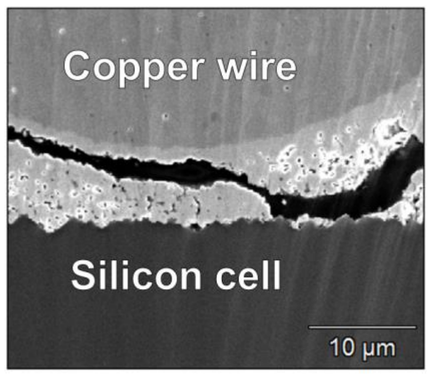

Fig. 2. Cross-section of cracked multiwire solder joint in a commercial module subjected to dynamic mechanical loading.

Thermomechanical fatigue lifetime assessments of prominent solder alloys, such as Sn-Pb and SAC, have been conducted largely through the Norris-Landzberg model [16]. Developed in 1969 at IBM for electronics packaging, the Norris-Landzberg model calculates the acceleration factor, or ratio of expected lifetimes between two thermal cycles as,

$$AF = f^{-m} \cdot \Delta T^{-n} \cdot \mathrm{f}(T_{max}) \tag{1}$$

where AF is the acceleration factor, f is the ratio of the test thermal cycling frequency to the field frequency, is the ratio of the test thermal cycling temperature differential to the field differential, $\mathrm{f}(T_{max})$ is an Arrhenius term depending on the maximum cycle temperature, and m and n are material dependent exponents for frequency and temperature, respectively. This model has been used extensively in microelectronics packaging and power electronics reliability studies and has been validated by experimental data for many solder alloys under a range of conditions, where it is widely accepted that m=1/3 and n=2 for eutectic SnPb solder [17, 18, 19, 20]. The Norris-Landzberg model has also been used to understand the thermomechanical fatigue lifetime of Sn-Pb solder joints in PV modules and to establish equivalency between lab testing and field deployment [6, 21]. An advantage of the Norris-Landzberg model is that the material parameters m and n can be derived from thermal cycles that do not strictly represent field conditions. The acceleration behavior can thus be assessed based on the relative fatigue lifetimes under various thermal cycling conditions.

In this work, the thermomechanical fatigue resistance of the low temperature solders InSn, SnBi, and SnBiAg are examined and compared to that of SnPb using an approach based on the Norris-Landzberg model. Test structures containing 30 solder joints were created for each of the four solders and for three different thermal cycling profiles. The crack growth was quantified using c-mode scanning acoustic microscopy (C-SAM) such that the change in failure rates with distinct thermal profiles was examined for each solder. Probability distributions were used to characterize the failure distributions and estimate lifetimes. The results show that although accelerated thermal cycling may be a meaningful qualification test for In-Sn alloys as well as for SnPb, multiwire products using Sn-Bi alloys require distinct accelerated testing due to distinct failure modes.

2. Experimental Methods

In order to accelerate solder damage, thermomechanical fatigue test samples were designed to have significant mismatch in the coefficient of thermal expansion (CTE). Each sample thus consisted of 30 11mm-diameter copper cylinders (CTE of 16.7 ppm/˚C) soldered to a direct bond copper (DBC) substrate, which has an effective CTE of 6.1 ppm/˚C. Copper substrates were chosen to mimic the copper wires used in the multiwire designs. Furthermore, copper is known to have high diffusivity and to readily form brittle intermetallic compounds, so the copper-solder interface is expected to pose a higher reliability risk than the solder-gridline interface. A schematic of one solder joint is shown in Fig. 3. The four solder alloys chosen for this study included three low temperature solders and eutectic SnPb for comparison (Table I). While InSn has the lowest eutectic temperature, it is more costly than the Sn-Bi alloys. Substrates and cylinders were cleaned in solvent and then in 5% HCl acid to remove oxides before reflow and solder flux was also used during reflow. The solder alloys were reflowed to about 20˚C above their eutectic temperatures under N_2 and then under vacuum to reduce voiding. The samples were subjected to three distinct thermal cycling profiles (Table II), where cycle length includes heating, cooling, and dwell times. Temperature was monitored via sample substrates and the dwell times were 5 minutes for all profiles. These thermal cycles were chosen to induce a reasonable amount of damage such that the fatigue lifetimes could be compared. The comparison of fatigue liftetimes under various thermal cycles allows for examination of the thermomechanical fatigue acceleration behavior. The samples were imaged via C-mode scanning acoustic microscopy with a Sonoscan® Gen5™ C-SAM® to measure the crack growth. The thermal cycling profiles range from more (TC-1) to less intense (TC-3).

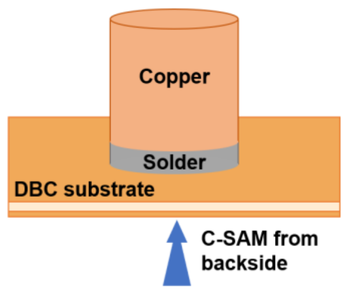

Fig. 3. Schematic of test structure design with one solder joint.

TABLE I. CHARACTERISTICS OF SOLDER ALLOYS UNDER INVESTIGATION [22]

Solder	Composition	Eutectic Temp. (˚C)	CTE (ppm/˚C)
SnPb	63-37	183	21
InSn	52-48	118	11
SnBi	42-58	139	14.5
SnBiAg	42-57-1	--	--

TABLE II. THERMAL CYCLING PARAMETERS

Thermal Cycle	Ramp Rate	Temperature	ΔT (˚C)	Cycle length (mins.)
TC-1	Fast ramp	High ΔT	-40˚ to +85˚	60
TC-2	Slow ramp	High ΔT	-40˚ to +85˚	101
TC-3	Slow ramp	Low ΔT	-22˚ to +67˚	90

The results are plotted on log-normal probability plots, where the y-axis is the normal probability scale as percents and the x-axis is the logarithm of the cycles to reach the failure criterion. These plots demonstrate the probability distributions of the failure data, allowing for comparison of the full datasets. A failure criterion of 5 mm^2 is used throughout, as this was the maximum amount of damage achieved by the majority of joints in each sample. Other failure criteria down to 2 mm^2 were examined and demonstrated the same trends presented here.

3. Results

3.1. Quantifying Crack Growth

Fig. 4a and 4b demonstrate the progression of crack growth as monitored by C-SAM. Fig. 4a shows the initial voids as bright white shapes, with the light area around the edges indicating very early phases of a crack. Fig. 4b shows the same joint 2900 thermal cycles later, where the edges of the joint have cracked appreciably. The reflected acoustic waves are disrupted at the cracked interface, such that the cracked area appears light while the intact areas remain dark. The void size and location are unaffected by thermal cycling. Fig. 4c shows a representative cross-sectional SEM image, confirming significant cracking through the solder interface. All cracking observed via cross-sections or by detached cylinders was found to be cohesive. A Python script was used for image analysis and the growth of cracked area throughout thermal cycling was identified by the increasing light areas in the C-SAM images.

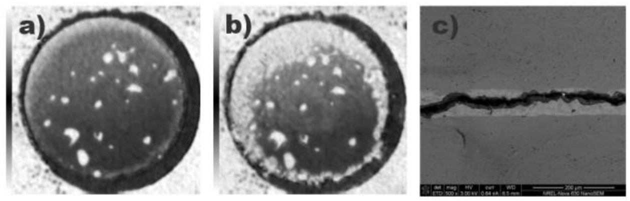

Fig. 4. C-SAM image of a SnBi solder joint after a) 1000 thermal cycles (TC) and b) 3900TC; c) SEM cross-section of a separate joint demonstrating cohesive cracking through the solder layer.

Fig. 5 shows a plot of the crack growth in each solder joint from the Sn-Bi, TC-1 sample over thermal cycling with a chosen failure criterion of 5 mm^2 cracked area, indicated by a dotted line. The cycles to fail for each joint are then extracted, removing outliers with a z-score greater than 2. The probability distributions are then represented on normal probability plots. This is repeated for each thermal cycling profile and for each solder alloy.

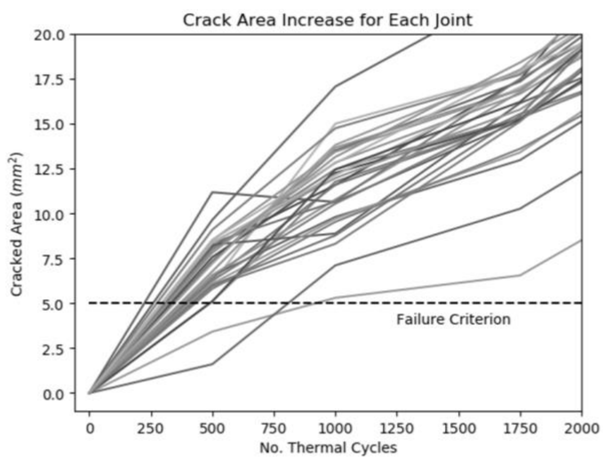

Fig. 5. Crack growth increase with thermal cycling for the thirty Sn-Bi solder joints subjected to TC-1. The impact of the failure criterion is demonstrated by the dotted line chosen where the cracked area is 5 mm^2.

For all solder types, Fig. 6 shows the average growth in cracked area under thermal cycling for TC-1 (a) and TC-3 (b). It can be seen from the shaded regions, representing one standard deviation, that the dataset has high variability, especially for the more intense thermal cycle. This variability likely stems from the initial sample quality, where nonuniformities in the solder joints would increase the data scatter. These samples involve large area solder bonds, and although voiding was minimized through bond surface preparation and a vacuum reflow step, there was clear variation from joint to joint in terms of initial voiding. Other nonuniformities, such as trapped flux byproducts, bondline thickness, or intermetallic compound growth may have also been present. While the samples designed for this study (Fig. 3) allowed for clear crack analysis due to the large bond area, more uniform sample quality could be achieved through sample designs that are more representative of the configuration within a PV module.

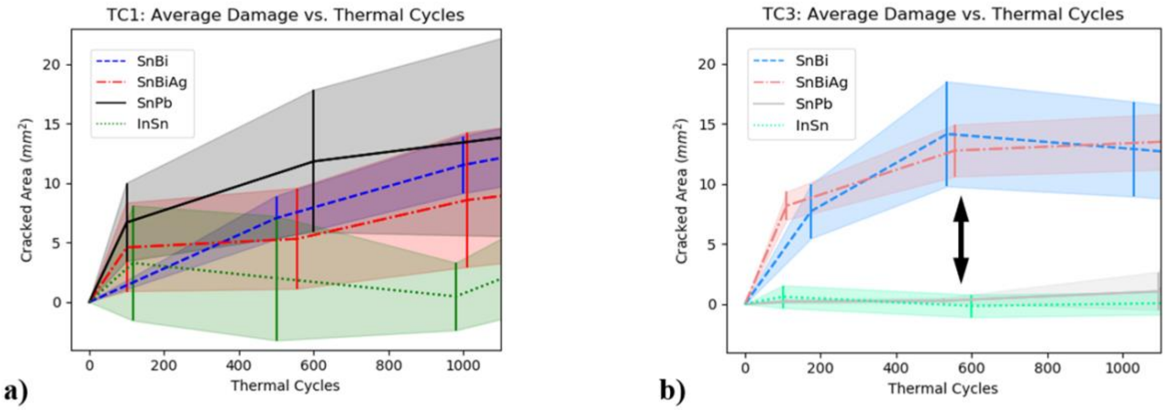

Fig. 6. Average crack area growth versus thermal cycles for a) TC1 and b) TC3. Shaded regions indicate the standard deviation. Results from TC1 (a) show high variability with all solder alloys in a similar range. Results from TC3 (b) indicate significant differences in damage accumulation for Sn-Bi alloys.

Despite the significant variability, qualitative comparisons can be made. Fig. 6 demonstrates that although the low temperature solders appear to have comparable performance to SnPb under the harsher cycle TC-1 (Fig. 6a), the Sn-Bi alloys continue to show significant cracking under the less intense TC-3 (Fig. 6b). In fact, the crack growth rate appears to be slightly higher for the Sn-Bi alloys under TC-3 versus TC-1, while InSn and SnPb experience significantly less damage under TC-3 compared to under TC-1.

3.2 Probability Distributions

The log-normal probability plots for SnPb and InSn are shown in Fig. 7. These plots show that the lifetime distributions shift to higher values with less intense thermal cycling. The probability plots for SnBi and SnBiAg are shown in Fig. 8 and show conversely that the lifetime distributions shift to lower values with less intense thermal cycling.

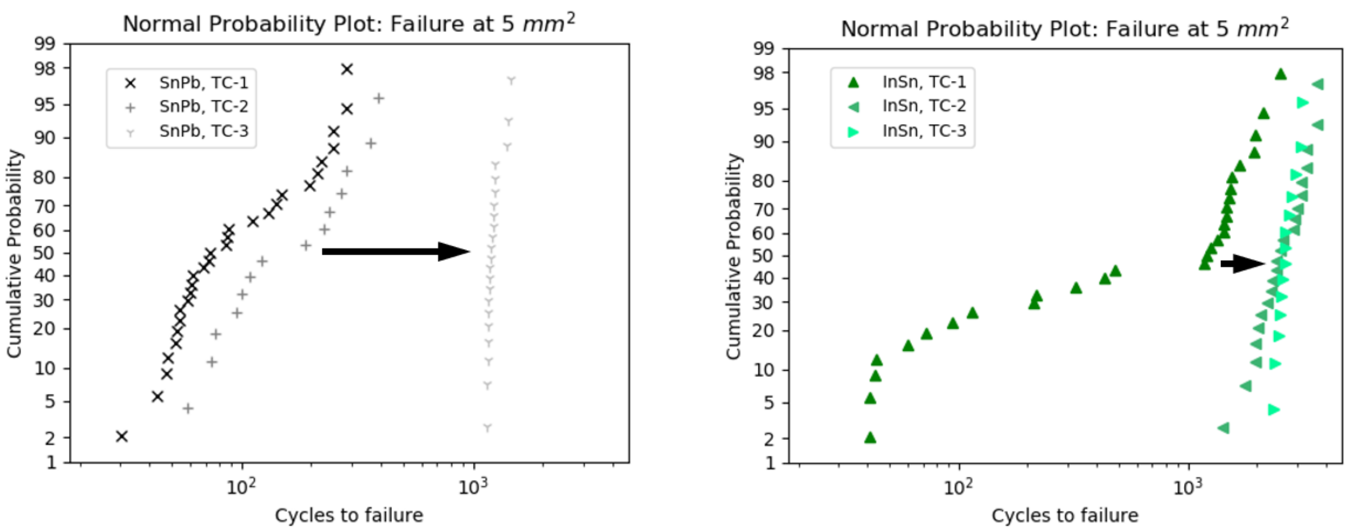

Fig. 7. Probability distributions for SnPb (left) and InSn (right) for all three thermal cycling profiles. Decreasing thermal cycle intensity increases lifetime.

The nonlinear appearances of the probability distributions, most apparent in the TC-1 results, indicate that the distributions are not well behaved. The aberrations lessen when the failure criterion is increased however, indicating that these nonlinearities are related to differences in early stage crack growth, most pronounced under the harshest thermal cycle. These differences may also be traced to initial sample quality and underscore the importance of considering data scatter in further quantitative analysis, such as mean lifetime or acceleration factor calculations.

Qualitatively, the trends in Fig. 7 are similar for both SnPb and InSn, where the lifetime decreases as thermal cycling intensity increases. It is also shown that SnPb is more significantly affected by the change in the thermal cycling temperature differential, while InSn is more affected by the change in thermal cycling frequency. In contrast to conventional Sn-Pb alloys, the Sn-Bi alloys demonstrate remarkable decreases in lifetime with decreasing thermal cycle intensity in Fig. 8.

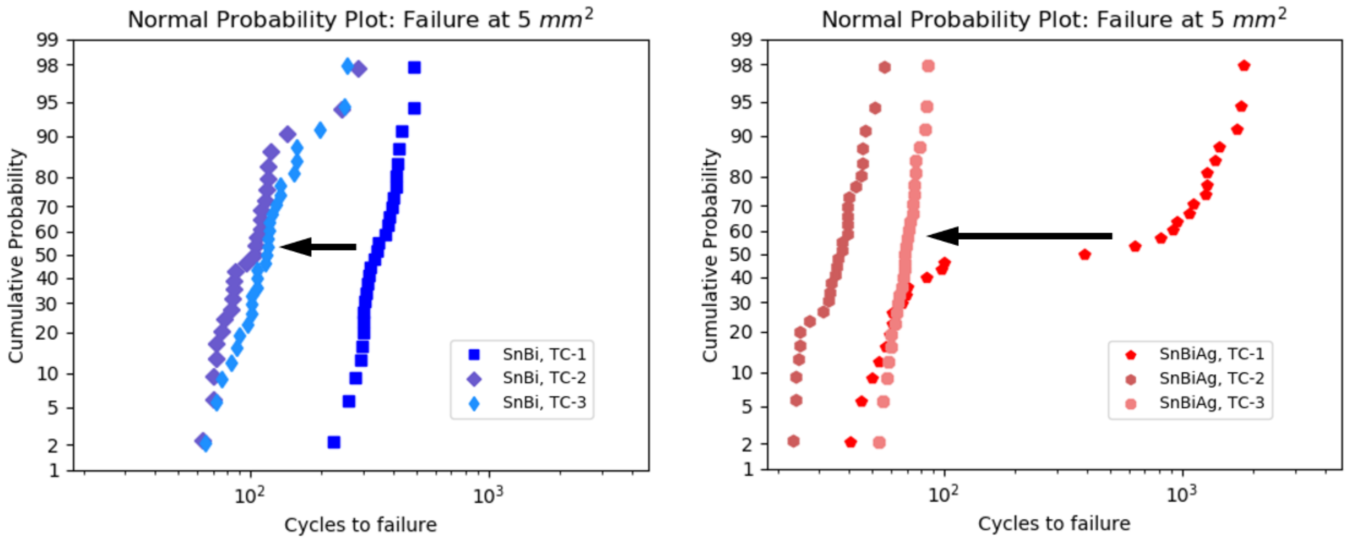

Fig. 8. Probability distributions for SnBi (left) and SnBiAg (right) for all three thermal cycling profiles. Decreasing thermal cycle intensity decreases lifetime.

There is some improvement in the fatigue lifetimes from TC-2 to TC-3 for both SnBi and SnBiAg, but these lifetimes are still much lower than the lifetimes under TC-1. This indicates that the Sn-Bi alloy acceleration behavior is significantly different from the conventional SnPb or the more costly InSn. Furthermore, the large difference between the lifetimes under the faster ramp cycle, TC-1, and the slower ramp cycles indicates higher sensitivity to the thermal cycling frequency than to the thermal cycling temperature differential for the Sn-Bi alloys. Given that the cycling frequency of TC-3 is slightly higher than that of TC-2 (Table II), slightly higher lifetimes may then be expected for TC-3.

4. ANALYSIS

4.1 Interpretation of Lifetime Trends

Fig. 7 demonstrates the higher sensitivity of the SnPb lifetimes to the thermal cycling temperature differential than to the thermal cycling frequency. This is qualitatively consistent with the known and widely used calculation of SnPb acceleration factors, where increasing the temperature differential accelerates damage significantly more than increasing cycling frequency [16], [19]. The results from SnPb and InSn both show that increased temperature differential and frequency accelerate the thermomechanical fatigue cracking, indicating that SnPb and InSn can be accelerated through conventional thermal cycling protocols. However, SnBi and SnBiAg demonstrate an opposite trend, where increasing frequency and temperature increase lifetime. Unusual fatigue behavior for Sn-Bi alloys has been noted before. Sato et al. demonstrated that elevated temperature unexpectedly improved SnBi fatigue lifetime under cyclic mechanical strain, possibly due to increased ductility [23]. The trends demonstrated in this study for Sn-Bi alloys indicate that the thermomechanical fatigue resistance at field conditions would be even lower than that shown here under TC-2 or TC-3. The Sn-Bi alloys have demonstrated high sensitivity to cycling frequency, and field conditions will have significantly lower thermal cycling frequency than the thermal cycles used here.

4.2 Implications for Accelerated Testing

While these materials are known to be sensitive to processing conditions and the test sample processing was not identical to that of module construction, extrapolation of the demonstrated trends indicates that the thermomechanical fatigue resistance of the Sn-Bi alloys will be quite poor at field conditions. These results also indicate that acceleration factors for Sn-Bi alloys would be less than one, meaning that more damage is expected at field conditions than in accelerated thermal cycling tests This is an important result, as it indicates that comparable performance for multiwire modules using Sn-Bi alloys and conventional modules under a TC200 exposure cannot be interpreted as comparable performance under field conditions. This is demonstrated in Fig. 9, where the solders are compared under TC-1 and then under the less-accelerated TC-3. Under TC-1, the more intense thermal cycle, the low temperature solder alloys slightly outperform SnPb. Yet under TC-3, the less intense thermal cycle, SnPb demonstrates a mean lifetime an order of magnitude higher than that of the Sn-Bi alloys. This demonstrates the importance of obtaining acceleration factors for new materials and architectures in order to accurately interpret accelerated testing and design meaningful tests for a given module construction.

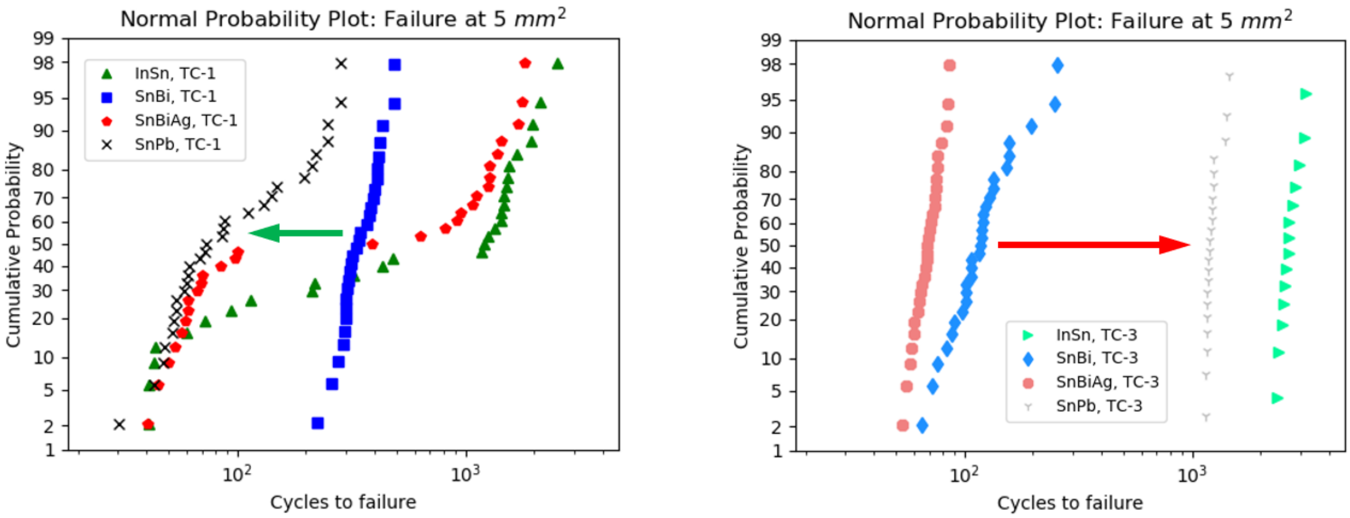

Fig. 9. Comparison of the four solder alloys under a high intensity thermal cycle (TC-1, left) and a low intensity thermal cycle (TC-3, right). The Sn-Bi alloys appear to outperform SnPb under TC-1 but have lower lifetimes than SnPb under TC-3 by an order of magnitude.

In this study the solder alloy is bonded to a copper substrate, as is the case in multiwire designs using solder-coated copper wires (Fig. 2). The solder is also bonded to silver gridlines, a coupling which may be more or less resistant to thermomechanical fatigue. However, the poor thermomechanical fatigue resistance for the copper-SnBi case presented here would prevent significant solder joint durability, regardless of the performance of the silver-SnBi case.

Despite the poor thermomechanical fatigue resistance of Sn-Bi alloys, multiwire interconnects still hold some promise. There are no documented cases of fielded multiwire modules with premature failures and failures have not been identified under lab testing [8, 24]. Accelerated thermal cycling under IEC 61215 requires even lower cycling frequencies than those used in this study, yet multiwire modules are able to withstand this exposure without significant power loss [25]. Thus, there is reason to believe that the primary contacting mode of the unique multiwire design is not metallurgical joints, which would be susceptible to thermomechanical fatigue, but instead mechanical contacts. Mechanical contacting could be enabled by the high redundancy of the contacting scheme and the novel processing involving lamination of the multiwire foil.

5 Conclusions

The thermomechanical fatigue resistance of low temperature solder alloys was assessed and compared to that of SnPb. The acceleration trends for SnPb were qualitatively as expected in terms of response to temperature and frequency, validating the experimental approach. InSn was shown to have acceptable thermomechanical fatigue resistance and acceleration on the order of that of SnPb but is costly and not currently favored in commercial products. Conversely, the lifetime trends for Sn-Bi alloys demonstrate that at field conditions the thermomechanical fatigue resistance is expected to be poor. The Sn-Bi alloys were also found to have thermal cycling acceleration factors of less than one, indicating that multiwire modules employing Sn-Bi alloys require distinct accelerated testing protocols from that of conventional modules. Significantly, this also indicates that standard approaches to accelerated testing may produce misleading results for emerging interconnect technologies without proper acceleration factors and understanding of the underlying failure mechanisms.

However, it has been suggested that the novel multiwire interconnect design does not require metallurgical joints, and that mechanical contacts may suffice for these design schemes. In this case, the failure mechanism is likely to be mechanical wear out of the contacts rather than thermomechanical fatigue. Further study of the contact wear-out is required, including material-level wear characterization and module-level cyclic mechanical loading. These investigations could be used to establish equivalencies to field conditions and understand the impact on performance and power output.

Acknowledgment

This work was authored by the National Renewable Energy Laboratory, operated by Alliance for Sustainable Energy, LLC, for the U.S. Department of Energy (DOE) under Contract No. DE-AC36-08GO28308. Funding provided by the U.S. Department of Energy Office of Energy Efficiency and Renewable Energy Solar Energy Technologies Office. The views expressed in the article do not necessarily represent the views of the DOE or the U.S. Government. The U.S. Government retains and the publisher, by accepting the article for publication, acknowledges that the U.S. Government retains a nonexclusive, paid-up, irrevocable, worldwide license to publish or reproduce the published form of this work, or allow others to do so, for U.S. Government purposes. The authors would like to thank Joshua Major for maintaining the C-SAM and reflow oven, Derek

Holsapple for performing C-SAM measurements, Dr. Ingrid Repins for helpful discussions, and Patrick Walker and Bobby To for SEM imaging.

REFERENCES

[1] C. Kanchanomai, Y. Miyashita and Y. Mutoh, "Low cycle fatigue behavior and mechanisms of a eutectic Sn-Pb solder 63Sn/37Pb," *Int J Fatigue,* vol. 24, no. 6, pp. 671-683, 2002.

[2] H. Ma and J. Suhling, "A review of mechanical properties of lead-free solders for electronic packaging," *J Mater Sci,* vol. 44, pp. 1141-1158, 2009.

[3] E. H. Amalu, D. J. Hughes, F. Nabhani and J. Winter, "Thermo-mechanical deformation degradation of crystalline silicon photovoltaic (c-Si PV) module in operation," *Engineering Failure Analysis,* vol. 84, pp. 229-246, 2018.

[4] M. T. Zarmai, N. N. Ekere, C. F. Oduoza and H. Amalu, "Evaluation of thermo-mechanical damage and fatigue life of solar cell solder interconnections," *Robotics and Computer-Integrated Manufacturing,* vol. 47, pp. 37-43, 2017.

[5] N. Bosco, T. J. Silverman and S. Kurtz, "The Influence of PV Module Materials and Design on Solder Joint Thermal Fatigue Durability," *Journal of Photovoltaics,* vol. 6, no. 6, pp. 1407-1412, 2016.

[6] N. Bosco, T. J. Silverman and S. Kurtz, "Climate specific thermomechanical fatigue of flat plate photovoltaic module solder joints," *Microelectronics Reliability,* vol. 62, pp. 124-129, 2016.

[7] J. Govaerts, T. Borgers, R. Van Dyck, N. Andries, P. Meyers, A. van der Heide, L. Vastmans, R. Moors, G. Doumen, P. Nivelle, M. Daenen, E. Voroshazi, C. Arnett, R. Labie, M. Van den Storme, G. Van den Storme, M. Dekens, S. Vandebroek, P. Schroyen, K. Smeers, T. Vavilkin, S. Dewallef, F. Abgrall, D. Jousset and J. Poortmans, "Encapsulant-Integrated Interconnection of Bifacial Solar Cells for BIPV Applications: Latest Results in the Twill-BIPV Project," in *Eur. PV Solar Energy Conf. (EUPVSEC)*, virtual, 2020.

[8] A. Faes, M. Depeisse, J. Levrat, J. Champliaud, N. Badel and M. Kiaee, "Smartwire Solar Cell Interconnection Technology," in *Proc. 29th EUPVSEC*, Amsterdam, 2014.

[9] A. Faes, M. Despeisse, J. Levrat and a. et, "Advanced Metallization Enabled by Smart-Wire Interconnection for Silicon Heterojunction Cells," in *Metal. Interconnect. Wksp.*, Konstanz, 2015.

[10] D.-Y. Shin, J.-R. Lim, W. Shin, C.-G. Lee and G.-H. Kang, "Single-Step Fabrication of a Photovoltaic Module Using Encapsulants with Low Melting Temperature Metal Ribbons Embedded," in *Eur. PV Solar Energy Conf. (EUPVSEC)*, virtual, 2020.

[11] G. Cattaneo, A. Faes, V. Barth, H.-Y. Li, J. Levrat, A. Bettinelli, L. Sicot, A. Richter, F. Rametta, C. Colletti, M. Izzi, M. Despeisse and C. Ballif, "Interconnection Technologies for High Reliable Bifacial Heterojuntion Glass/Glass Photovoltaic Modules," in *Eur. PV Solar Energy Conf. (EUPVSEC)*, virtual, 2020.

[12] N. Pujari, S. Sarkar and C. Bilgrien, "Low Temperature Lead Free Solder Pastes for Shingling Interconnection," in *Eur. PV Solar Energy Conf. (EUPVSEC)*, virtual, 2020.

[13] J. Sayeddi, "Thermal fatigue behavior of low melting point solder joints," *Soldering & Surface Mount Tech,* vol. 5, no. 1, pp. 26-32, 1993.

[14] J. Glazer, "Metallurgy of low temperature Pb-free solders for electronic assembly," *International materials reviews,* vol. 40, no. 2, pp. 65-93, 1995.

[15] G. Ren, I. J. Wilding and M. N. Collins, "Alloying influences on low melt temperature SnZn and SnBi solder alloys for electronic interconnections," *J Alloys Compounds,* vol. 665, pp. 251-260, 2016.

[16] K. C. Norris and A. H. Landzberg, "Reliability of Controlled Collapse Interconnections," *IBM J. Res. Develop.,* vol. 13, pp. 266-271, 1969.

[17] P. Lall, A. Shiragaokar and D. Arunachalam, "Norris–Landzberg Acceleration Factors and Goldmann Constants for SAC305 Lead-Free Electronics," *J. Electron. Packaging,* vol. 134, pp. 031008-1-12, 2012.

[18] O. Salmela, "Acceleration factors of lead-free solder materials," *IEEE Trans. Compon. Packaging Manuf. Tech.,* vol. 30, no. 4, pp. 700-707, 2007.

[19] J. Arnold, N. Blattau, C. Hillman and K. Sweatman, "Reliability Testing of Ni-Modified SnCu and SAC305 - Accelerated Thermal Cycling," in *Surf. Mount Tech. Assn (SMTA) Int.*, Orlando, 2008.

[20] V. Vasudevan and X. Fan, "An acceleration model for lead-free (SAC) solder joint reliability under thermal cycling," in *Proc. IEEE Electron. Compon. Tech. Conf.*, 2008.

[21] S. . M. Dasari, K. V. Nagaraj, S. Saravanan, P. Suratkar and T. K. Prasad, "Studying the lifetime of crystalline PV modules by interpreting acceleration test data with statistical reliability models," *Photovoltaics International,* vol. 15, pp. 141-147, 2012.

[22] M. Abtew and G. Selvaduray, "Lead-free Solders in Microelectronics," *Mat. Sci. Eng.,* vol. 27, pp. 95-141, 2000.

[23] T. Sato, Y. Kariya and K. Fukui, "Effect of temperature and strain rate on low-cycle fatigue life of Bi-Sn eutectic alloy," in *Proc. ASME InterPACK*, Burlingame, CA, 2013.

[24] A. Waltinger, H. Mehlich, J. Hausmann, T. Kluge, M. Heinrich, S. Hanni, A. Richter, A. Faes and D. Andronikov, "Endurance of Smart Wires," in *9th SOPHIA PV-Module Reliability Workshop*, 2019.

[25] T. Soderstrom, Y. Yao, R. Grischke, M. Gragert, B. Demaurex, B. Strahm, P. Papet, H. Mehlich, M. Koenig, A. Waltinger, J. Zhao and J. Krause, "Low cost high energy yield solar module lines and its applications," in *IEEE Photovolt. Spec. Conf. (PVSC)*, 2015.